

CFD MODELING OF SMOKE REVERSAL

C. C. Hwang and J. C. Edwards
NIOSH/ Pittsburgh Research Laboratory
Pittsburgh, PA 15236

ABSTRACT

In the design for a fire or smoke emergency, a main concern is maintaining an evacuation path that is free of smoke and hot gases. In ventilated tunnel fires, smoke and hot gases may form a layer near the ceiling and flow in the direction opposite to the ventilation stream. The existence of the reverse stratified flow has an important bearing on fire fighting and evacuation of underground mine roadways, tunnels, and building corridors. In the present study, a computational fluid dynamics (CFD) program is used as a design tool to model floor-level fires in a ventilated tunnel. The fire is simulated by a diffusion flame of propane issuing from a circular hole on the tunnel floor. The computed profiles of velocity and temperature along channel cross sections are similar to those obtained experimentally. The computed reverse-flow layer length has been correlated with a densimetric Froude number with some success. A non-dimensional parameter involving the source fire intensity is also used for the correlation. These analyses show that an appropriate ventilation air current must be maintained to provide an evacuation path from the source fire clear of smoke and hot gases. It is believed that CFD modeling, employed correctly and interpreted carefully, can be a useful design tool for fire protection.

INTRODUCTION

Although there has been increased attention to life safety during fire emergency in tunnels and mine roadways, there is no universally accepted design and operation of life safety systems for fire emergencies. In ventilated tunnel fires, smoke and other combustion products have been observed to fill the tunnel for a considerable distance on the intake side of a fire. Under certain flow and fire conditions, smoke may form a layer near the ceiling and flow in the direction opposite to the ventilation stream. The existence of reverse stratified layer of hot combustion products has an important bearing on fire fighting and evacuation of underground mine roadways, tunnels, and building corridors. It is of practical importance to understand the physical parameters and flow conditions under which the reverse stratified flow occurs.

In the design for a fire or smoke emergency, a main concern is maintaining an evacuation path that is free of smoke and hot gases. Consider a scenario involving a stopped vehicle on fire in a tunnel, disrupting traffic and requiring worker and passenger evacuation. Another scenario involves a conveyer-belt fire in an underground mine entry, producing smoke and toxic combustion products. The design must focus on determining the ventilation required to maintain a single evacuation path from the fire source clear of smoke and hot gases. The risk from accidental fires as well as the subsequent smoke movement depends largely on these applied ventilation currents.

When a fire is started on the floor of a straight channel without a ventilation (cross) flow, a hot plume rises above the fire and entrains the surrounding cold air into the plume. The plume, reaching the ceiling, forms two equal gas streams flowing in the opposite direction along the ceiling. The hot ceiling layer carries with it heat, carbon monoxide, smoke, and other combustion products. These layering streams eventually lose their buoyancy through heat loss to the strata or to the air beneath. The flow field is symmetric with respect to the plume axis. When a cross ventilation current exists, the symmetry in the rising plume and in the ceiling gas streams no longer exists. The ventilation current bends the plume and the length of the ceiling layer flowing against the ventilation current is reduced. It can be expected that the length of the hot ceiling layer is a function of the fire intensity and the ventilation velocity. The temperature of the layer decreases as the gas flows away from the region where the plume impinges the ceiling. Two mechanisms contribute to the temperature decrease. One mechanism is the heat losses of the layer along the ceiling, and the other is cooling resulting from entraining the surrounding cold air into the layer. As a result, the temperature at the front region of the layer reaches the surrounding air temperature and the layer loses its buoyancy and identity.

Previous workers employed simple empirical models to specify the critical velocity needed to prevent upstream movement of smoke from a fire in a tunnel [1-6]. In general, these models consider the buoyancy head and the dynamic head in the system, and deduce appropriate quantities for correlation. Hwang et al. [7], Daish & Linden [8] and Charters et al. [9] employed phenomenological models that provide more detail than the simple empirical approaches. A recent review of tunnel fires by Grant et al. [10] pointed out that existing experimental data still show an inadequate fundamental understanding of the interaction between buoyancy-driven combustion products and forced ventilation, the validity of extrapolating small-scale results to large scales, the influence of slopes on smoke movement and the effect of tunnel geometry. They also pointed out that CFD-based models represent the best way forward for prediction purposes, because CFD models make few prior assumptions about the gross flow character. CFD models are based on the fundamental conservation equations in fluid mechanics, and provide, in theory, fine resolution of the problem in terms of both space and time for all the parameters of interest. With increasing availability of powerful computers, considerable attentions are given to CFD modeling of fire in buildings and ventilated tunnels [11-16].

In the present study, a CFD program is used as a design tool to model floor-level fires in a ventilated tunnel. The fire is simulated by a reacting fuel issuing from a hole on the floor of a channel. The shape of the hole may be circular or rectangular. The tunnel has a rectangular cross section with sufficient length upstream to accommodate formation of reverse-layer flow. The fire is simulated by a diffusion flame of propane (mass fraction unity) issuing from a circular hole on the tunnel floor. A commercial program CFD2000 by Adaptive Research¹ is employed for the flow field computations. A four-step finite rate reaction scheme is used to represent a realistic fire-ventilation interaction in the plume zone. The standard k- ϵ turbulence model is used in the three-dimensional channel flow. The subsequent development of hot-gas layers is three-dimensional. Re-circulating flow patterns, movement of the ceiling-layer front, and distributions of gas temperature and velocity are studied under various fire parameters.

¹ Reference to a specific product does not imply endorsement by NIOSH.

MODEL DESCRIPTION

The governing equations for the flow field are expressed as partial differential equations.
mass conservation

$$\frac{\partial \rho}{\partial t} + \frac{\partial(\rho U_i)}{\partial x_i} = 0 \quad (0.1)$$

$$\text{momentum conservation} \quad \frac{\partial(\rho U_i)}{\partial t} + \frac{\partial(\rho U_i U_j)}{\partial x_j} = -\frac{\partial p}{\partial x_i} - \frac{\partial \tau_{ij}}{\partial x_j} + S_{U_i} \quad (0.2)$$

$$\text{energy conservation} \quad \frac{\partial h}{\partial t} + \frac{\partial(\rho U_j h)}{\partial x_j} = \frac{\partial p}{\partial t} + U_j \frac{\partial p}{\partial x_j} + \frac{\partial}{\partial x_j} \left[\left(\frac{\mu}{\text{Pr}} + \frac{\mu_t}{\text{Pr}_t} \right) \frac{\partial h}{\partial x_j} \right] + S_h \quad (0.3)$$

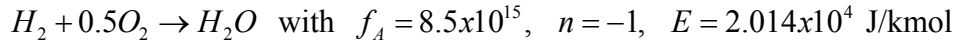
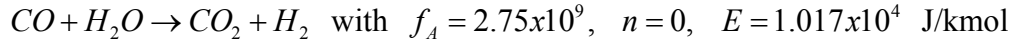
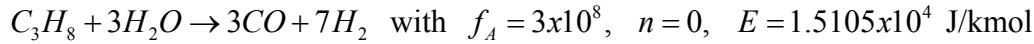
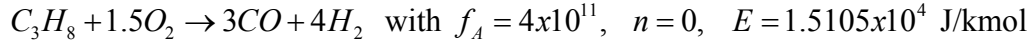
$$\text{species conservation} \quad \frac{\partial \rho Y_i}{\partial t} + \frac{\partial(\rho U_j Y_i)}{\partial x_j} = \frac{\partial}{\partial x_j} \left[\left(\frac{\mu}{\text{Sc}} + \frac{\mu_t}{\text{Sc}_t} \right) \frac{\partial Y_i}{\partial x_j} \right] + \dot{\omega} \quad (0.4)$$

$$\text{gas equation of state} \quad p = \frac{R}{M} T \quad (0.5)$$

or turbulence modeling, the standard two-equation $k - \varepsilon$ turbulence model was employed [17], in which additional equations for the kinetic energy of turbulent fluctuations (k) and the rate of dissipation of turbulence energy (ε) are solved. The empirical constants appearing in the equations are $c_\mu = 0.09$, $c_1 = 1.44$, $c_2 = 1.92$, $\text{Pr}_k = 1.0$, $\text{Pr}_\varepsilon = 1.3$. This set of constants is adopted from Launder and Spalding [17]. It may be noted that a modified $k - \varepsilon$ model has been used by Woodburn & Britter [14] to include the effects of buoyancy and wall damping on the turbulence. The following boundary conditions are used in this work. At the upstream (inflow) side of the channel, a uniform air velocity u_{in} is specified (forced ventilation) with $v = 0$ and $w = 0$. The entering air temperature T_{in} is 300K and for the entering species the mass fractions are $Y_{O_2} = 0.233$, $Y_{N_2} = 0.767$, $Y = 0$ for other species. For the turbulence inlet conditions, $k_{in} = 0.02 \text{ m}^2 / \text{s}^3$ and $\varepsilon_{in} = 0.02 \text{ m}^3 / \text{s}^3$. At the downstream (outflow) side of the channel a uniform pressure is specified. The value of u_{out} is computed and no-source condition is specified for the other variables. The channel walls are assumed to be impervious, adiabatic, and non-slip. A program-supplied turbulence wall function is used. The modeling of a floor fire and its boundary conditions are described in the next section.

Modeling a Floor Fire

The fuel employed in the reaction process is propane (C_3H_8). To realistically simulate the burning process, the fuel reacts with air in a 4-step finite rate reaction scheme as shown in the following equations [18]:



where f_A is the Arrhenius coefficient, n is the collision factor exponent, and E is the activation energy. The number of the chemical species involved are C_3H_8 , O_2 , H_2 , CO , CO_2 , H_2O , and N_2 . At the source fire, the mass fractions of all species are zero except that of C_3H_8 which is set $Y_{C_3H_8} = 1.0$. The fuel velocity w_{in} is taken to be 0.1-0.3 m/s ($u = 0$, $v = 0$) and $T = 1200$ K. The fuel velocity is approximately equal to the burning rate of the liquid fuels in open trays [19].

RESULTS AND DISCUSSION

The channel used in the modeling is 30 m long, 2.4 m wide, and 1.6 m high. For fixed channel geometry, the main parameters considered are the ventilation velocity u_{in} , the fuel-exit velocity w_{in} , the fuel-exit diameter, and the channel inclination angle. The quantity w_{in} is proportional to the rate of heat generation at the source fire. The fuel exits from a 0.8-m (or 0.4-m) diameter floor opening located at a distance 10 m from one end of the channel where ventilation air enters. Figure 1 shows the geometry of the channel with grid distribution. A three-dimensional body-fitted grid with $49 \times 13 \times 17$ cells in the tunnel length, width and height direction was used for the 0.8-m diameter fire. For the 0.4-m diameter fire, a grid with $51 \times 13 \times 18$ cells was used. When the reverse flow layer length exceeds 8 m, the ventilation flow was admitted from the end with a 20-m leading distance to the fuel exit. It is assumed that the flow development at the entrance region has negligible effect on the flow reversal of the layer.

The results are based on the computed flow field 30 seconds after the initiation of the fire. An initial plume rises to the ceiling and hot ceiling layers evolve during a transition period. It appears that the flow field has attained a steady state at this time. When a reverse flow layer occurs, as shown in Fig. 2 the contour of zero axial velocity in channel cross sections upstream of the plume is approximately parallel to the ceiling. This confirms an experimental observation that smoke layers are of uniform thickness at a channel cross section. This implies that the flow along the ceiling layer is approximately two-dimensional. This observation may prompt a theoretician to approach the problem using a simplified analysis. In Fig. 2 the velocity vectors are also shown. It is noted that the magnitude of the vectors shown represents the component of the total vector in the y-z plane, and that the x-component of the velocity across the contour of $U = 0$ changes its sign. The hot gas in the central region of the layer flows into the ventilation

current below and a less amount of cold airflows into the layer near the wall regions. As a result the layer loses its buoyancy.

The computed profiles of velocity and temperature along channel cross sections are shown in Figs. 3 and 4. These profiles are similar to those obtained experimentally in a fire tunnel by Hwang and Wargo [20]. Figure 5 shows vector plots in the $x-z$ plane at $y=0$ as a function of u_{in} . As the value of u_{in} increases, the length of the reverse stratified layer decreases because of the increased counteracting effects of the ventilation current.

The channel inclination has considerable effects on the layer length of a reverse flow. When the ventilation flow has an upward component (positive inclination represented by $+\phi$), keeping other conditions fixed, the reverse-flow layer length decreases. When the ventilation flow has a downward component, the reverse-flow length increases. The computed reverse-flow layer length has been correlated with a densimetric Froude number Fr with some success (Fig. 6). In Fig. 6, Fr is defined by

$$Fr = \frac{(\rho_{in} - \rho_{c,\min})gH}{\rho_{in}u_{in}^2},$$

where $\rho_{c,\min}$ is the smallest value of the gas density in the ceiling layer. This corresponds to the highest temperature along the ceiling and is found at the region where the rising plume impinges on the ceiling. On the physical ground, $\rho_{c,\min}$ represents the product of an interaction of a rising plume with a fire strength \dot{Q} and a ventilation current with an average velocity u_{in} . As shown in Fig. 6, the effect of the channel inclination ϕ is so pronounced that it is shown using separate lines. The effect of the size of the fuel exit (size of the source fire) on the reverse-layer length has been included by a parameter $(D/W)^{1/2}$. The application of this type of correlation to a fire protection design needs the information on $\rho_{c,\min}$ which cannot be found *a priori*, though some estimate may be made from experimental data taken under similar conditions.

A non-dimensional parameter involving the fire source intensity is also used for correlating the computed reverse-flow layer length L . The relevant non-dimensional parameters are taken as

$$\frac{L}{H} = f\left(\frac{\dot{Q}}{A_{in}u_{in}^3\rho_{in}}, \frac{gH}{c_p(T_f - T_{in})}, \phi\right) \quad (0.6)$$

The first term in the bracket is the ratio of heat generation by the fire to the kinetic energy of the ventilation current. The second term in the bracket is the ratio of the potential energy to the thermal energy of the rising gas from the fire. The parameter ϕ is the channel inclination angle. In Figure 7 the reverse-layer length is correlated with the fire strength and the channel-inclination angle, where

$$X = \left(\frac{\dot{Q}}{A_{in}u_{in}^3\rho_{in}}\right)^{0.947}$$

and

$$Y = \frac{L}{H} \left(\frac{gH}{c_p(T_f - T_{in})} \right)^{0.398} (1 - (\sin \phi)^{1/3})^{-1.705}$$

In this correlation, the experimental data of Guelzim et al. [4] are also included. In their small-scale experiment a 3 m long half cylinder with an inside diameter of 0.3 m was used to simulate an arched tunnel. Midway along the tunnel a propane gas burner 2 cm in diameter was located. Forced ventilation was imposed with a variable rotation speed fan. It is seen that the effect of ϕ is successfully included in the correlation.

To determine the ventilation required to maintain a single evacuation path from the fire source clear of smoke and hot gases, we may set $\frac{L}{H}=0$ in Figure 7 and solve for u_{in} . This value of u_{in} is the critical ventilation velocity. From the correlation in Figure 7 it is determined that the critical velocity is proportional to the heat rate to the one-third power.

CONCLUSIONS

A CFD code based on the standard $k - \varepsilon$ turbulence model was used to model a floor-level fire in a ventilated channel. The result of computations showed a qualitative behavior of the movement of the combustion products in the fire channel. The profiles of the gas velocity and temperature along channel cross sections are similar to those experimentally observed.

The inclusion of a finite-rate reaction scheme resulted in very long computations. It may be possible to employ a simpler reaction scheme (such as the mixture-fraction model) and simulate a realistic fire scenario. This point requires further investigations.

The present computations use a constant value of pressure at the channel exit and a uniform flow of ventilation air velocity at the channel entrance. In a real fire scenario, fans drive the ventilation air, and as a fire develops, the ventilation current is reduced because of an increased flow resistance in the channel. Thus, the boundary conditions used in the present computations apply to the fire scenario at the steady state.

In various analytical and experimental investigations, the tunnel shapes and sizes will vary considerably. Because of the lack of geometrical similarity among various studies, caution should be exercised in the comparison of results obtained under dissimilar geometries. The same caution applies to the cases with dissimilar fire scenarios.

It has been shown how CFD analysis can be used to determine a correlation between smoke reversal length and tunnel ventilation. The resultant correlation can be used to provide guidance for smoke management control measures. For example, the correlations indicate that ventilation current proportional to the one third power of the fire intensity must be maintained to provide an evacuation path from the fire source clear of smoke and hot gases. This is an example of how a CFD modeling employed correctly and interpreted carefully, can be a useful design tool for fire

protection. Future investigation with other CFD codes and additional experiments should result in improved reverse flow length correlations.

NOMENCLATURE

A	area, m^2	T	local fluid temperature, K
c_p	specific heat, J/kg/K	t	time, s
D	diameter of fuel exit, m	U_i	i th-fluid velocity component, m/s
E	activation energy, J/kmol	u	x -component of velocity, m/s
Fr	Froude number	v	y -component of velocity, m/s
f_A	Arrhenius coefficient	w	z -component of velocity, m/s
g	gravitational acceleration, m/s^2	W	channel width, m
h	specific enthalpy, J/kg	x_i	position vector in the i th coordinate direction, m
H	channel height, m	Y_i	mass fraction of species i
L	length of reverse stratified layer, m	ρ	local fluid density, kg/m^3
M	molecular weight, kg/kmol	μ	laminar dynamic viscosity, $N \cdot s/m^2$
n	collision factor exponent	μ_t	turbulent dynamic viscosity, $N \cdot s/m^2$
p	fluid pressure, N/m^2	$\dot{\omega}$	species production rate, $kg/s \cdot m^3$
Pr	laminar Prandtl number	$\tau_{i,j}$	viscous stress tensor, N/m^2
Pr_t	turbulent Prandtl number		
\dot{Q}	rate of heat generation, kJ/s	<u>Subscripts</u>	
R	universal gas constant, J/kmol/K	a	air
Sc	laminar Schmidt number	c	ceiling
Sc_t	turbulent Schmidt number	f	fuel
S_h	heat production per unit volume	in	entering
S_{U_i}	i th component of body force per unit volume (e.g., gravity)	min	minimum

REFERENCES

1. Thomas, P.H., "Movement of Smoke in Horizontal Corridors against an Air Flow," *Inst. Fire Engrs Q.*, Vol. 30, pp. 45-53, 1970.
2. Hinckley, P.L., "The Flow of Hot Gases along an Enclosed Shopping Mall: a Tentative Theory," *Fire Research Note No. 807*, Fire Research Station, 1970.
3. Heselden, A.J.M., "Studies of Fire and Smoke Behavior Relevant to Tunnels," *Proc. 2nd Int. Symp. On the Aerodynamics and Ventilation of Vehicle Tunnels*, Cambridge, UK, pp. 23-25, March 1976, BHRA Fluid Engineering, 1976.
4. Guelzim, A., Souil, J.M., Vantelon, J.P., Sou, D.K., Gabay, D., and Dallest, D., 1994, "Modelling of a Reverse Layer of Fire-Induced Smoke in a Tunnel," *Fire Safety Science – Proceedings of the Fourth International Symposium*, pp. 277-288.
5. Kennedy, W.D., Gonzales, J.A., and Sanchez, J.G., "Derivation and Application of the SES Critical Velocity Equations," *ASHRAE Transactions: Research*, Vol. 102, no.2, pp. 40-44, 1996.
6. Oka, Y., Atkinson, G.T., "Control of Smoke Flow in Tunnel Fires," *Fire Safety JI* Vol. 25, pp. 305-322, 1996.
7. Hwang, C.C., Chaiken, R.F., Singer, J.M., and Chi, D.N.H., "Reverse Stratified Flow in Duct Fires: Two-Dimensional Approach," *16th Symposium (International) on Combustion*, pp. 1385-1395, The Combustion Institute, Pittsburgh, PA, 1977.

8. Daish, N.C. & Linden, P.F., "Interim Validation of Tunnel Fire Consequence Models: Comparison between the Phase 1 Trials Data and the CREC/HSE Near-Fire Model," *Cambridge Environmental Research consultants Report No. FM88/92/6*, 1994.
9. Charters, D.A., Gray, W.A. & McIntosh, A.C., "A Computer Model to Assess Fire Hazards in Tunnels (FASIT)," *Fire Technol.*, Vol. 30, 134-154, 1994.
10. Grant, G.B., Jagger, S.F., and Lea, G.J., "Fires in Tunnels," *Phil. Trans. R. Soc. Lond.*, A 356, pp. 2873-2906, 1998.
11. Kumar, S. and Cox, G., "Mathematical Modelling of Fires in Road Tunnels," *Proc. Of 5th Int. Symp. on the Aerodynamics and Ventilation of Vehicle Tunnels*, Paper B1, Lille, France, 20-22 May, 1985.
12. Simcox, S., Wilkes, N.S., & Jones, I.P., "Computer Simulation of the Flows of Hot Gases from Fire at King's Cross Underground Station," *Fire Safety Journal*, Vol. 18, pp. 49-82, 1992.
13. Rhodes, N., "Review of Tunnel fire and Smoke Simulations," *Proc. Of 8th Int. Conf. On the Aerodynamics and Ventilation of Vehicle Tunnels*, pp. 471-486, 6-8 July, Liverpool, 1994.
14. Woodburn, P.J. and Britter, R.E., "CFD Simulation of a Tunnel Fire – Part I," *Fire Safety Journal*, Vol. 26, pp.35-62, 1996.
15. Lea, C.J., Owens, M. & Jones, I.P., "Computational Fluid dynamics Modelling of Fire on a One-third Scale Model of a Channel Tunnel Heavy Goods Vehicle Shuttle," *Proc. Of 9th Int. Conf. on Aerodynamics and Ventilation of Vehicle Tunnels*, pp.681-692, 6-8 October, Aosta Valley, Italy, 1997.
16. Edwards, J.C. and Hwang, C.C., "CFD Analysis of Mine Fire Smoke Spread and Reverse Flow Conditions," *Proceedings of the 8th U.S. Mine Ventilation Symposium*, pp. 417-422, 1999.
17. Launder, B.E. and Spalding, D.B., "The Numerical Computation of Turbulent Flow," *Comp. Mech. In Appl. Mech. and Engr.*, Vol. 3, pp.269-289, 1974.
18. Jones, W.P. and Lindstedt, R.P., "Global Reaction Schemes for Hydrocarbon Combustion," *Comb. & Flame*, Vol. 73, p. 233, 1988.
19. Burgess, D.S., Grumer, J. and Wolfhard, H.G., "Burning Rates of Liquid Fuels in Large and Small Open Trays," *Int. Symp. On the Use of Models in Fire Research*, Nat. Acad. of Sci.-Nat. Res. Council Publication 786, 1961.
20. Hwang, C.C. and Wargo, J.D., "Experimental Study of Thermally Generated Reverse Stratified Layers in a Fire Tunnel," *Combustion and Flame*, V.66, pp.171-180, 1986.

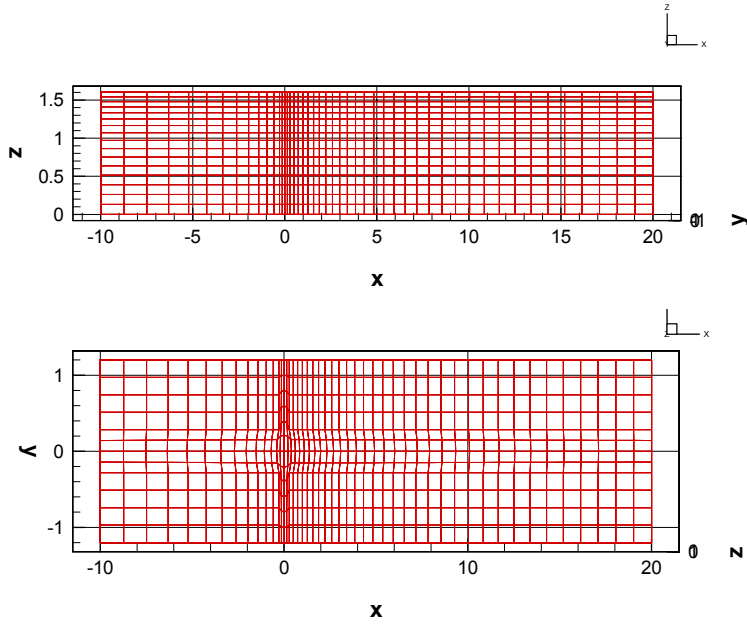


Figure 1. Channel geometry and grid distribution

$u_{in} = 0.5 \text{ m/s}$, $w_{in} = 0.2 \text{ m/s}$, $\phi = 0^\circ$
 cut plane $x = -1 \text{ m}$
 contour of u

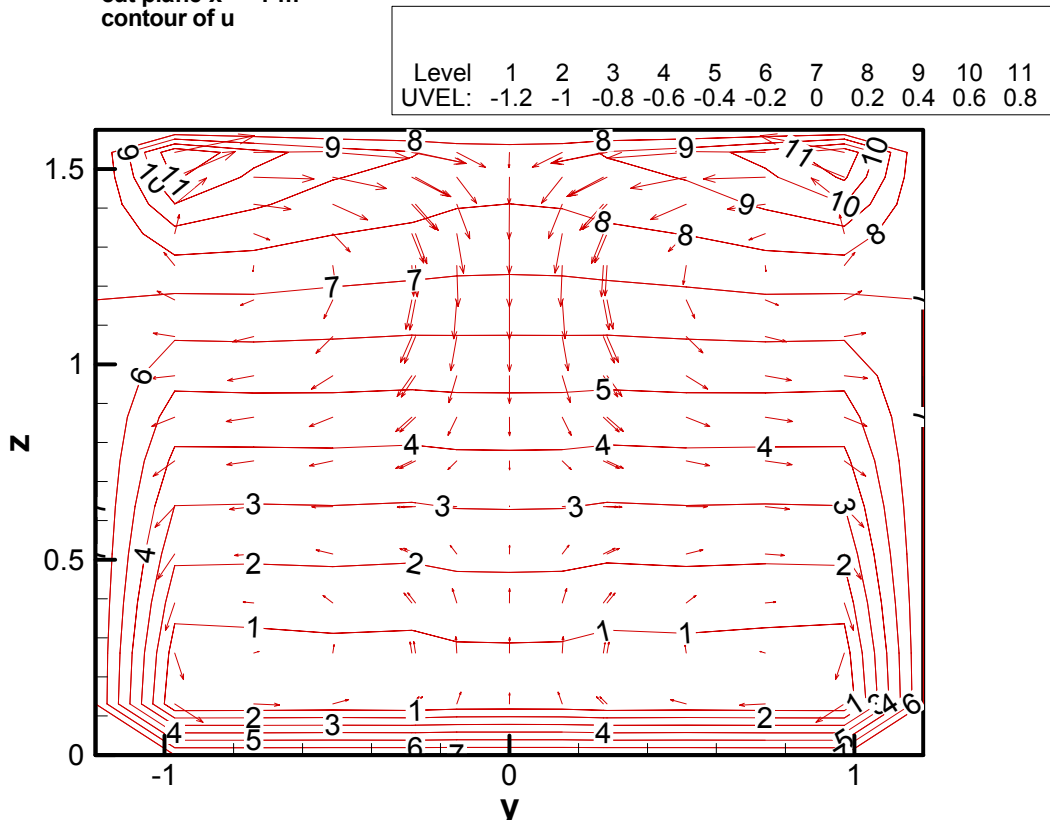


Figure 2. The contour of the axial velocity in the channel cross-section at $x = -1 \text{ m}$. The region above level 7 is a reverse stratified layer.

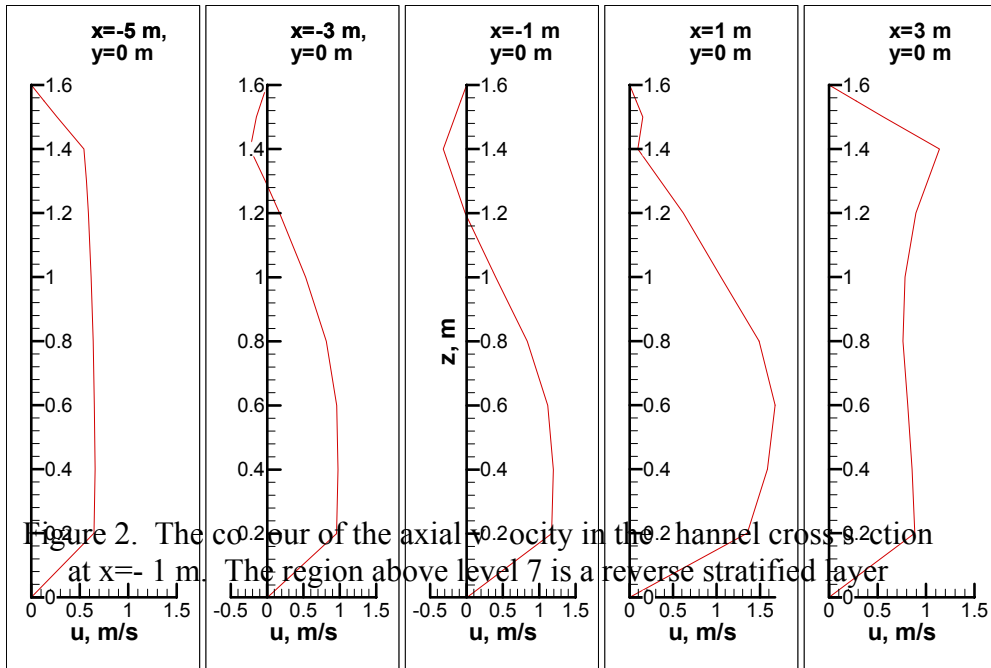


Figure 3. Velocity distribution along z (height) in the plane $y=0$, at various values of x (axial distance).

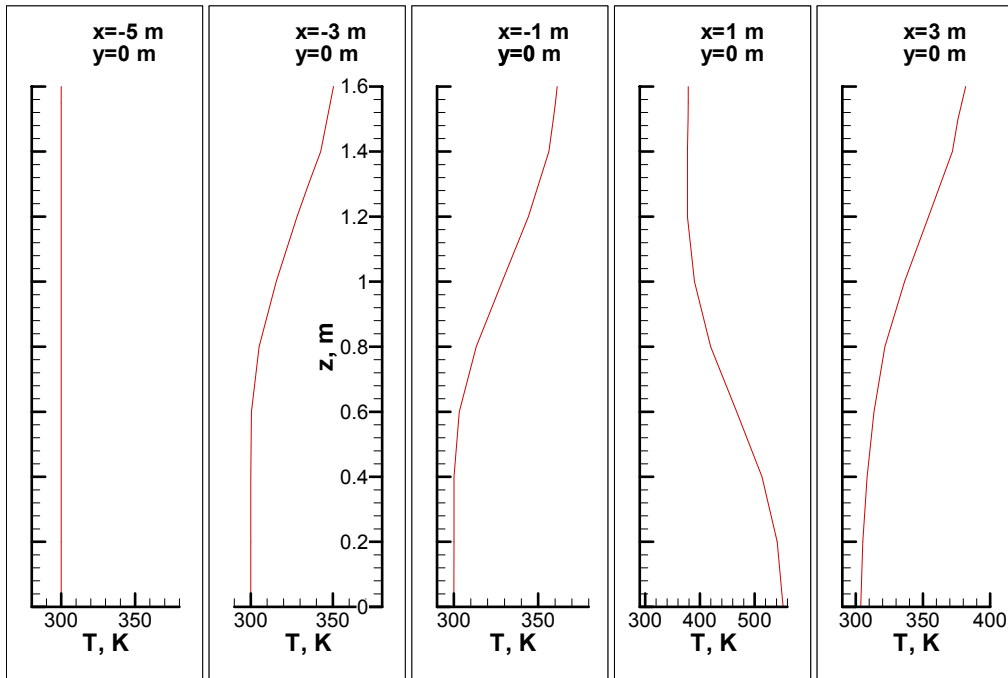


Figure 4. Temperature distribution along z (height) in the plane $y=0$ at various values of x (axial position).

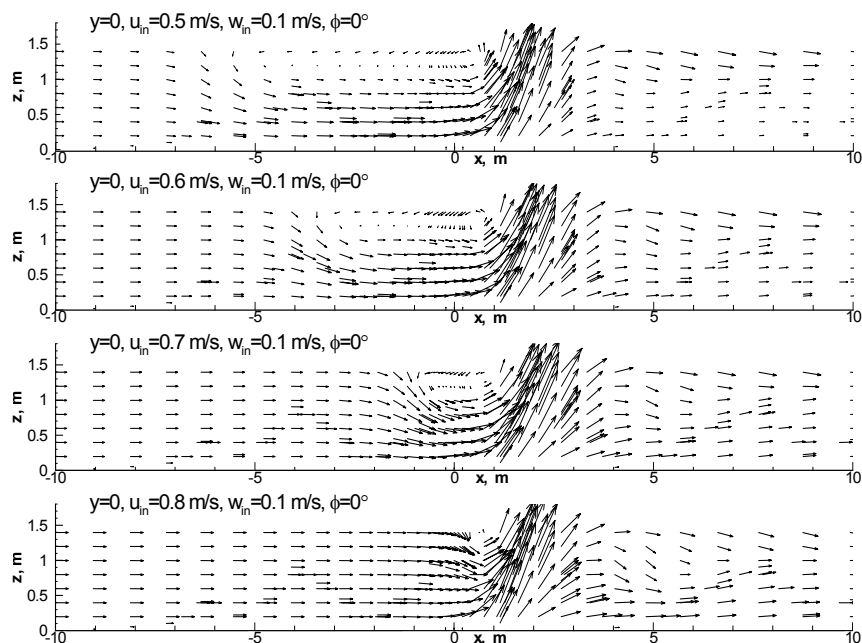


Figure 5. Velocity vector plots showing the extent of reverse stratified layers for various flow conditions.

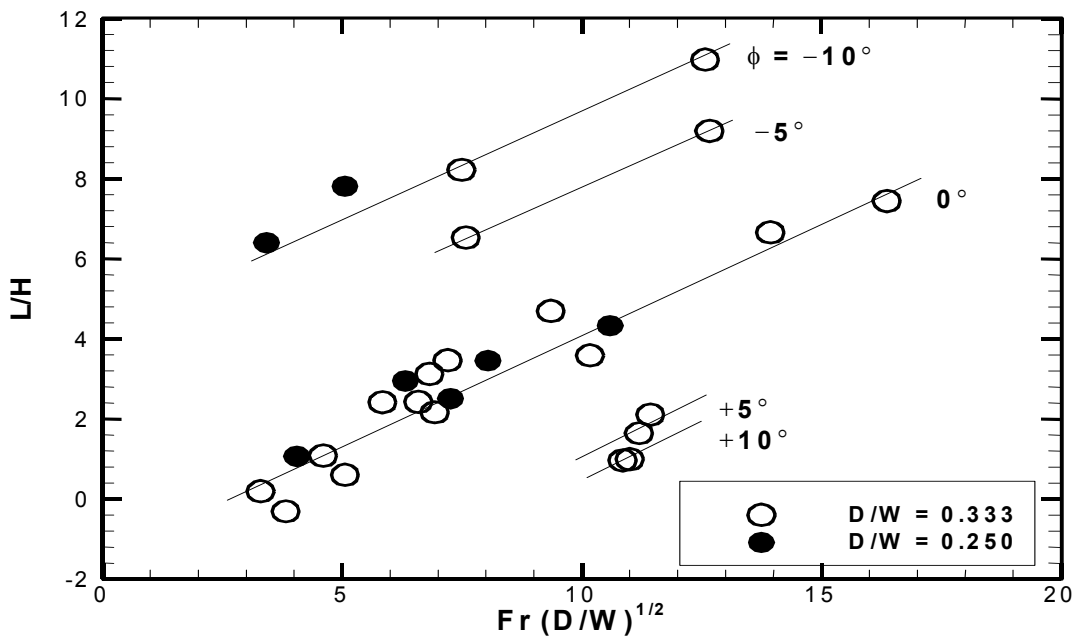


Figure 6. $\frac{L}{H}$ versus $Fr(D/W)^{1/2}$ for different values of the channel inclination angle ϕ .

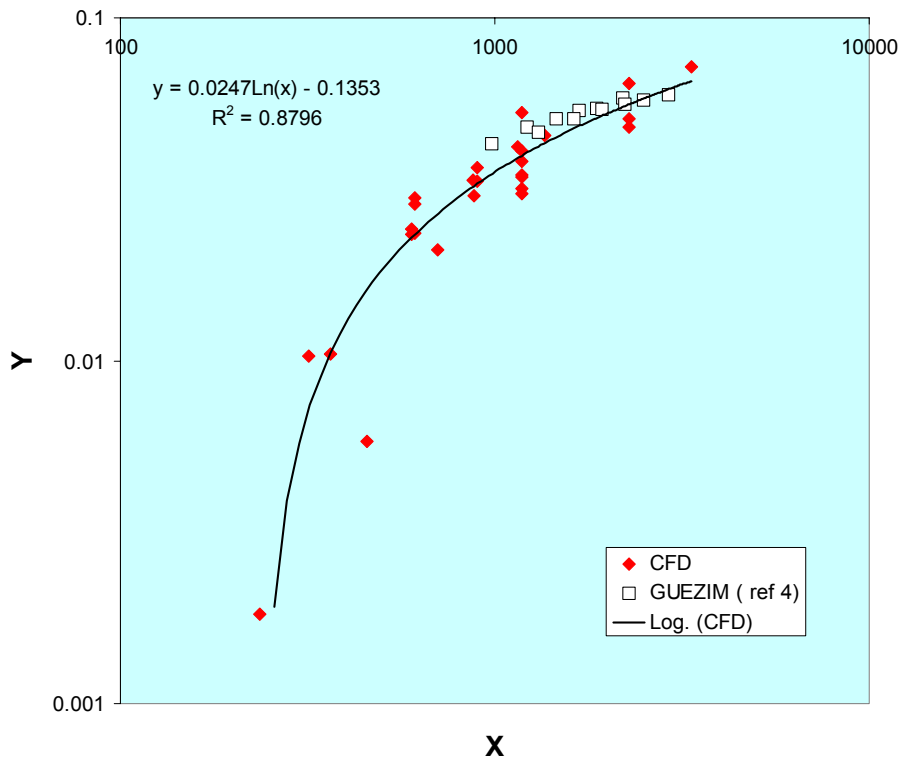


Figure 7. A correlation using parameters X and Y .